

Dynamic topology optimization of structure weakly coupled with two-phase flow

Gil Ho Yoon

School of Mechanical Engineering, Hanyang University, Seoul, South Korea

ARTICLE INFO

Keywords:

Topology optimization
Two-phase flow in container
Monolithic design approach
Phase-field method
Transient sensitivity analysis

ABSTRACT

This study presents a new topology optimization method for transient two-phase fluid-structure interaction (FSI) problem. From a topology optimization point of view, it is formidable challenging to consider the mutual coupling with structure and two-phase flow and the evolution of sharp interface between two-phase flow (tracking interface). To tackle these formidable issues, the monolithic design approach incorporating with the deformation tensor is applied and the simulation of the two-phase flow is carried out with the volume of fluid (VOF). The spatially varying design variables in topology optimization determines whether the corresponding domains or elements are solid or fluid (two-phase flow) to maximize or minimize objective function. To simplify the coupling procedure and maintain the numerical convergence, the one-way coupling between two-phase fluid and structure is assumed rather than the two-way coupling. To carry out the topology optimization, the Darcy's force determined by the design variable is added to the Navier-Stokes equation and the Young's modulus and the structural density are also interpolated with respect to the design variables. In addition, the phase-field equation in the VOF method is also modified to take into account the evolution of the design variable and the front of the phase field value. To investigate the effect of the two-phase fluid-structure interaction, several transient two-dimensional problems are considered.

1. Introduction

This study introduces a novel topology optimization approach to address the challenging problem of transient two-phase (biphase) fluid-structure interaction (FSI) as shown in Fig. 1 [1]. The inherent complexity of the present study lies in the intricate coupling between structure and two-phase flow as well as the dynamic evolution of the sharp interface between fluids (tracking interface). To tackle these formidable challenges, this study adopts the monolithic design approach, incorporating the deformation tensor, and simulating the two-phase fluid using the volume of fluid (VOF) method without considering the mixture of flow. To evaluate the impact of two-phase fluid-structure interaction, we consider transient simulation and optimization problem inside container.

Multiphase flow is a complex flow phenomenon involving the simultaneous movement of multiple distinct substances with different phases or aggregative states. A discrete phase can be solid, liquid and gaseous state and two phase flow is a special case of multiphase flow. From a simulation perspective, a phase can be characterized as a distinct portion of a substance in a system that possesses unique physical properties,

enabling its differentiation from other phases within multiphase system. Several innovative analysis studies can be found in [2–5]. One of the representative approaches is the volume of fluid (VOF) method with which the portion of material properties are computed with a continuous scalar function in analysis domain (See [2] and references therein). From an optimization of multiple phase flow point of view, several researches can be found [3–5]. In addition to the difficulties in the topology optimization for multiphase flow, the topology optimization for fluid-structure interaction system is also challenging.

Many researches are prevail for fluid topology optimization. The work by Borrvall and Petersson may be the first work which introduces the spatially varying porous domain for fluid topology optimization [6]. With the relatively large Darcy's force, the fluid velocity becomes zero that feature can be utilized for fluid topology optimization. Inspired by this concept, many innovative works have been presented [7–19] with a variety of flow conditions and numerical methods. However, it is still challenging to consider complex fluid-structure interaction phenomena in topology optimization. It is also possible to use the body fitted mesh with the explicit boundary with the level-set or the phase-field method [20]. For the fluid-structure interaction problem, the simulation

E-mail addresses: ghy@hanyang.ac.kr, gilho.yoon@gmail.com.

<https://doi.org/10.1016/j.compstruc.2024.107471>

Received 7 November 2023; Accepted 25 June 2024

Available online 17 July 2024

0045-7949/© 2024 Elsevier Ltd. All rights are reserved, including those for text and data mining, AI training, and similar technologies.

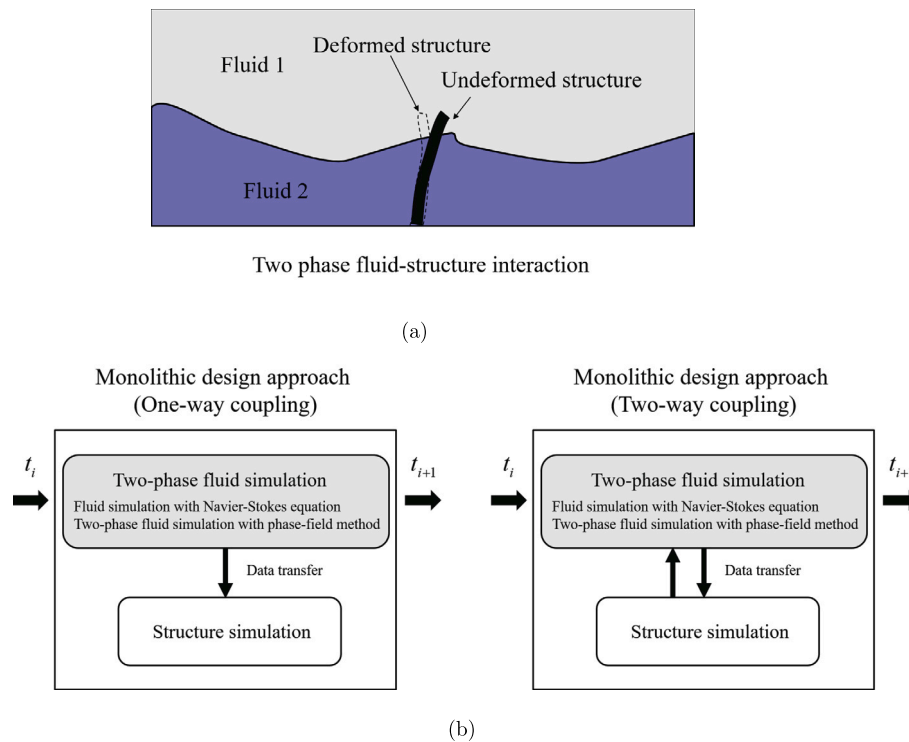


Fig. 1. (a) Topology optimization of two-phase fluid-structure interaction and (b) the one-way coupling theory (left) and the two-way coupling theory (right).

and optimization conditions become more perplex as the two governing equations should be considered. The two different strategies exist for topology optimization for fluid-structure interaction problem. The first strategy may be the approach with the distinct interface between FSI [21–24]. In [21,23,24], two and three dimensional FSI problems are considered with the level-set approach. In [22], the modified immersed finite element method and the meshfree reproducing kernel particle method are employed with the level-set approach for the topology optimization fluid-structure interaction. In [25], the topology optimization approach with the explicit levelset method and the extended FEM approach (XFEM-LSM) are presented and the concept of “wet” with non-determined FSI boundary and “dry” with the fixed explicit FSI boundary is discussed. In [26], the thermal fluid-structure system using body-fitted meshes is considered. In [27,28], the monolithic design approaches for compliance minimization and stress problem are presented. In [29], continuous two-phase fluid system is considered in topology optimization. As an extension, the present study expands toward the two-phase fluid-structure interaction system. In [30–32], the topology optimization for FSI with binary design variable and TOBS is developed. While reviewing the relevant researches, it is found that the topology optimization for biphasic FSI has not been researched before this. The biphasic FSI indicates a system with structure submerged inside two-phase fluids (gas-fluid or fluid-fluid). Inevitably, the computational procedure of the multiphysics system becomes complicated and its application for gradient based optimization is inherently challenging too. To our best knowledge, the study of this multiphysics system is rare and has not been researched.

This study introduces a novel topology optimization approach to address the challenging problem of transient two-phase fluid-structure interaction (FSI) as shown in Fig. 1 [1]. The transient two-phase fluid simulation is carried out first and the computational results of fluid velocities and pressure are utilized to formulate the fluid-structure interaction system as shown in Fig. 1. The inherent complexity of the present study lies in the intricate coupling between the structure and two-phase fluid and the dynamic evolution of the sharp interface between fluids (tracking interface). To tackle these formidable challenges, this study adopts the monolithic design approach, incorporating the de-

formation tensor, and simulate the two-phase fluid using the volume of fluid (VOF) method. Spatial design variables in topology optimization dictate whether corresponding domains or elements are solid or fluid (two-phase flow), thereby optimizing objective function. To ensure the numerical convergence, this study employs one-way coupling between the two-phase flow and structure instead of the two-way coupling approach. The topology optimization process involves augmenting Darcy’s force, determined by the design variable, into the Navier-Stokes equation, while also interpolating Young’s modulus and structural density with respect to the design variable. Furthermore, we modify the phase-field equation in the VOF method to account for the evolution of the design variable and the front of the phase field value. A transient adjoint approach for evaluating the sensitivity information is derived with a gradient-based optimizer.

The remainder of this paper is organized as follows. Section 2 provides the mathematical formula pertaining to the coupled analysis of the transient structure and two-phase transient flow motions and the development of the sensitivity analysis of the integration of the transient compliance. Section 3 describes several topology optimization examples that test the effect of a transient flow and demonstrate its importance. Section 4 presents the conclusions of the study and provides suggestions for future research.

2. One way coupling of two-phase(biphasic) fluid-structure interaction with the monolithic design approach

In this section, the theory of one way coupling of two-phase (biphasic) fluid-structure interaction with the monolithic design approach is developed and presented. In nature, the strong interplay and interdependency between structure and two-phase flows are observed. The theory explicated in [1] and [28] delves into the notion of the fully-strong coupling phenomenon for topology optimization for fully coupled fluid-structure interaction. In this research, we consider the one-way coupling due to the difficulties in the consideration of the structural displacements in the transient simulation of two-phase flow; this consideration stands distinct from the assumption of the small displacement in the monolithic design approach. To meticulously consider the two-phase

fluid simulation, the VOF (Volume-Of-Fluid) approach in connection to the phase field or the levelset approach is seamlessly incorporated. After simulating the transient two-phase flow, the rigorous structural analysis ensues.

2.1. Development of a new weakly fluid-structure interaction with two-phase flow

Two-phase flow equation

Transient fluid flow, governed by the momentum conservation equation, complies with the continuum condition and is influenced by the gravitational force, symbolized as $\rho\mathbf{g}$, and the force of surface tension, denoted as \mathbf{F}_{st} .

$$\rho \frac{\partial \mathbf{v}}{\partial t} + \rho(\mathbf{v} \cdot \nabla)\mathbf{v} = -\nabla p + \mu \nabla \cdot (\nabla \mathbf{v} + \nabla \mathbf{v}^T) \cdot \mathbf{v} + \rho\mathbf{g} + \mathbf{F}_{st}, \mathbf{v} = \mathbf{v}(\mathbf{x}, t) \quad (1)$$

$$\frac{\partial \rho}{\partial x} + \nabla \cdot (\rho \mathbf{v}) = 0 \quad (2)$$

where the fluid velocities and pressure are denoted by \mathbf{v} and p , respectively. In the absence of accounting for structural deformation, the spatial coordinate before structural deformation (\mathbf{X}) and the spatial coordinate after structural deformation (\mathbf{x}) remain indistinguishable, denoted as $\mathbf{x} = \mathbf{X}$. The viscosity and the density are denoted by μ and ρ , respectively. There are the gravity force (\mathbf{g}) and the surface tension force (\mathbf{F}_{st}) along the interface boundary. The Neumann and Dirichlet boundary conditions are assigned with the initial condition.

To emulate the metamorphosis of bi-phase fluid, the following phase field approach complemented with the re-initialization factor is implemented.

$$\frac{\partial \phi}{\partial t} + \mathbf{v} \cdot \nabla \phi - \gamma_L \nabla \cdot (\epsilon \nabla \phi + \phi(1 - \phi) \frac{\nabla \phi}{|\nabla \phi|}) = 0 \quad (3)$$

The parameter for the interface thickness and the re-initialization parameter are denoted by ϵ and γ_L . Having successfully resolved the aforementioned advection equation, the fluid within the domain of analysis is subsequently categorized as such:

$$\phi(\mathbf{x}, t) = \begin{cases} 0 & \text{if } \mathbf{x} \in \text{Fluid 1} \\ \text{Otherwise} & \text{if } \mathbf{x} \in \text{Interface boundary } \Gamma \\ 1 & \text{if } \mathbf{x} \in \text{Fluid 2} \end{cases} \quad (4)$$

where the interface boundary condition is defined by Γ defined inside the analysis domain. The Neumann boundary condition is applied for the phase field equation at the boundary. By employing the Continuum Surface Force model [5,33], it is possible to define the surface tension force, \mathbf{F}_{st} , as follows:

$$\mathbf{F}_{st} = \nabla \cdot [\sigma(\mathbf{I} - \mathbf{n}_{int} \mathbf{n}_{int}^T) \delta_{int}] \quad (5)$$

where the normal direction vector of the interface boundary is set to $\mathbf{n}_{int} = \frac{\nabla \phi}{|\nabla \phi|}$ and δ_{int} is defined as $6|\phi(1 - \phi)| |\nabla \phi|$. The surface tension coefficient is denoted by σ . Subsequently, the density and the viscosity are interpolated with respect to the normalized ϕ value, ϕ_n .

$$\phi_n = \min(\max(\phi, 0), 1) \quad (6)$$

$$\rho = \rho_1 + (\rho_2 - \rho_1)\phi_n \quad (7)$$

$$\mu = \mu_1 + (\mu_2 - \mu_1)\phi_n \quad (8)$$

where the density values of the first fluid and the second fluid are ρ_1 and ρ_2 , respectively and the viscosity values of the first fluid and the second fluid are μ_1 and μ_2 , respectively. The above equations are related and necessary for the simulation of two-phase fluid in the framework of the volume of fluid (VOF). The interpolation of the fluid properties is set by the value of the phase field value, ϕ . As it is related to the two-phase fluid simulation, the linear interpolation is carried out. Note that the above equations are related and necessary for the simulation of two-phase fluid in the framework of the volume of fluid (VOF). Note that

in the above equations, the structural displacements are not taken into account to consider the one-way coupling simulation. In reality, considering this mutual coupling is essential. However, due to simulation difficulties and the imposition of the small displacement condition, this research is limited to considering only one-way coupling.

Linear elasticity equation

With the one-way coupled fluid-structure interaction, the continuity in the traction force is imposed. To consider this continuity in FSI system, the monolithic design approach employs the transformation of the traction force into one formulated in the analysis domain. To achieve this, the deformed domain, ${}^t\Omega$, and the undeformed domain, ${}^0\Omega$, are distinguished and the deformation tensor, \mathbf{F} is employed.

$$\mathbf{F} = \frac{\partial \mathbf{x}}{\partial \mathbf{X}} \quad (9)$$

The positions of the undeformed domain, ${}^0\Omega$, and the deformed domain, ${}^t\Omega$, are denoted as \mathbf{X} and \mathbf{x} , respectively. The essential idea of the monolithic design approach is to apply the above deformation tensor to the differential and the integral operators.

$$\nabla_{\mathbf{x}} = \mathbf{F}^T \nabla_{\mathbf{x}}, \nabla_{\mathbf{x}} = \mathbf{F}^{-T} \nabla_{\mathbf{X}} \quad (10)$$

The governing equation of linear dynamic structure is defined as follows:

$$\nabla_{\mathbf{x}} \cdot \mathbf{T}_s + \mathbf{F} = \rho_s \ddot{\mathbf{u}} \text{ in } {}^t\Omega \quad (11)$$

where the structural stress tensor is represented as \mathbf{T}_s , while the displacements are denoted as \mathbf{u} . The force and inertial forces are represented as \mathbf{F} and $\rho_s \ddot{\mathbf{u}}$, respectively. The structural density is denoted by ρ_s .

2.2. Parameterization of the present governing equations with the density design variables

For the topology optimization with the spatially varying density design variables, the modifications of the above governing equations are necessary to reflect the evolution of the design variables considering the stability of the nonlinear equations in (1), (2), (3), and (11).

Navier-Stokes equation

To model the pseudo rigid domain in the fluid domain, the equation in (1) is modified as follows:

$$\rho \frac{\partial \mathbf{v}}{\partial t} + \rho(\mathbf{v} \cdot \nabla_{\mathbf{x}})\mathbf{v} = -\nabla p + \mu \nabla \cdot (\nabla_{\mathbf{x}} \mathbf{v} + \nabla_{\mathbf{x}} \mathbf{v}^T) \cdot \mathbf{v} + \rho\mathbf{g} + \mathbf{F}_{st} - \alpha \mathbf{v} \quad (12)$$

The fluid analysis domain is denoted as Ω_t , which simultaneously contains the two-phase flow equations and the elastodynamic equation. As the one-way weakly coupling is considered, the two domains of Ω_0 and Ω_t are not distinguished in the fluid domain. In the end of the transient two-phase Navier-Stokes equation, the Darcy force is added [6,13,15,34].

$$\alpha(\gamma_e) = \alpha_{\max} \gamma_e^{n_{pen}} \quad (13)$$

where the maximum coefficient and the penalization factor are denoted by α_{\max} and n_{pen} , respectively. The e -th design variable is denoted by γ_e . The mass conservation equation in (2) does not require a modification.

Phase-field equation

To improve the convergence and impose the pseudo rigid domain condition, the present paper modifies the phase-field equation in (3). From an equation point of view, as the fluid velocity becomes small enough, the value of the phase field equation is subjected to be fixed or the pseudo-rigid domain can be modeled. Note that regardless of the value of the phase-field equation, the phase field values of the pseudo-rigid domain become fixed. However, to improve the numerical convergence in this advection equation assuming the incompressibility, we propose the following modification by adding the penalization to the advection term.

$$\frac{\partial \phi}{\partial t} + \underbrace{(1-\gamma)}_{\text{Added Penalization}} \mathbf{v} \cdot \nabla \phi - \gamma_L \nabla \cdot (\epsilon \nabla \phi + \phi(1-\phi) \frac{\nabla \phi}{|\nabla \phi|}) = 0 \quad (14)$$

Note that the term \mathbf{v} is modified by multiplying $(1-\gamma)$; the penalization of the design variable is not attempted but it is conceived for the incorporation of the penalization. When the design variable γ becomes one or the corresponding domain is modeled with the pseudo-rigid domain not allowing the penetration of fluid, the velocity term \mathbf{v} becomes small enough to regard the corresponding region as the rigid domain. Therefore, in principle, this modification is not actually necessary. However, in connection to the structural equation, we observed that it helps the convergence of the nonlinear solver. It is also interesting to see that the domain with one for γ is regarded as the solid domain regardless of the value of the ϕ .

Linear elasticity equation

In the monolithic design approach for FSI, the coupling is carried out in a different method. The fluid equation and structural equation exist for an entire analysis domain (${}^0\Omega$ or ${}^t\Omega$). In the monolithic design approach, the weak form of the structural equation can be expressed as follows:

$$-\int_{0\Omega} \rho_s \delta \mathbf{u}^T \ddot{\mathbf{u}} - \int_{0\Omega} \delta \mathbf{S}^T \cdot \mathbf{T}_s d\Omega + \int_{0\Omega} \Psi \cdot \mathbf{F}^{-T} \delta \mathbf{S}(\mathbf{u}, \delta \mathbf{u})^T \cdot p \|\mathbf{F}\| d\Omega + \int_{0\Omega} \Psi \cdot \mathbf{F}^{-T} \delta \mathbf{u} \cdot \nabla_{\mathbf{x}} p \|\mathbf{F}\| d\Omega = 0 \quad (15)$$

$$\delta \mathbf{S} = \frac{1}{2} (\nabla_{\mathbf{x}} \delta \mathbf{u} + \nabla_{\mathbf{x}} \delta \mathbf{u}^T), \tilde{\mathbf{S}}(\mathbf{u}, \delta \mathbf{u}) = \frac{1}{2} (\nabla_{\mathbf{x}} \delta \mathbf{u} + \nabla_{\mathbf{x}} \delta \mathbf{u}^T) \quad (16)$$

The virtual displacements are denoted by $\delta \mathbf{u}$, and the virtual and auxiliary virtual strains are denoted by $\tilde{\mathbf{S}}$ and $\mathbf{S}(\mathbf{u}, \delta \mathbf{u})$, respectively. The mutual coupling condition from the point of view of the linear elastodynamic equation is imposed by divergence theory.

In the proposed monolithic design approach, the phase-field equation determining the kind of fluid and the fluid equation are formulated in an entire analysis domain (${}^0\Omega$ or ${}^t\Omega$). In the linear elasticity equation, the three parameters including the density and the Young's modulus and the window function, Ψ , are interpolated with respect to the design variables as follows:

$$\begin{aligned} C(\gamma_e) &= C_s \gamma_e^n + C_f (1 - \gamma_e^n) \\ \rho(\gamma_e) &= \rho_s \gamma_e^{n_s} + \rho_{void} (1 - \gamma_e^{n_s}), \rho_{void} \ll \rho_s \\ \Psi &= \gamma_e^{n_{filter}} \end{aligned} \quad (17)$$

where the Young's moduli of the structure and fluid are denoted as C_s and C_f , respectively. The density values of the structure and void are denoted as ρ_s and ρ_{void} , respectively. The penalization factors are denoted by n and n_s . To remove local oscillations, the value of n_s is set to be higher than that of n . Depending on the penalization factor, various local optima can be obtained. The window function Ψ is defined to convert the boundary integration (fluid force exerted on the structure) to domain integration. The penalization factor for the window is n_{filter} . In the present modeling, the void region inside structure is modeled with fluid. The one-way coupling from fluid to structure is assumed. The material interpolation of fluid and solid is not sufficient for the topology optimization for two phase fluid as the surface tension exists. The fact that the surface tension among fluids should be tracked and simulated by the evolution of the phase field smoothly is difficult and challenging. Some careful studies in choosing a proper combination of the parameters of the numerical methods are required as the time reversal scheme for the sensitivity analysis for the time integration objective function suffers from the non-convergence.

2.3. Optimization formulation for a new weakly fluid-structure interaction with two-phase flow

For the optimization formulation, the obvious choice may be the transient structural compliance. For dynamic system, the dynamic compliance which can be defined as the product of force and displacement can be considered. Therefore, in the present study, we propose to consider the time integration of the structural compliance as the objective function with the mass constraint as follows:

$$\begin{aligned} \text{Min}_{\gamma} \quad & J = \int_0^{t_f} \int_{0\Omega} \mathbf{S}^T \cdot \mathbf{T}_s d\Omega dt \\ \text{Subject to} \quad & \sum_{e=1}^{N_e} \gamma_e v_e \leq \text{mass}_0 \end{aligned} \quad (18)$$

$$\gamma = [\gamma_1, \gamma_2, \dots, \gamma_{N_e}], \quad \gamma_{\min} \leq \gamma \leq 1, \quad \gamma_{\min} = 0.001$$

where the simulation time is denoted by t_f and the element volume is denoted by v_e . The upper mass limit is denoted by mass_0 . The above integration over time and domain can be considered as the objective function. With the above objective function, the adjoint sensitivity analysis procedure is applied for the transient multiphysics system.

$$\begin{aligned} \mathcal{L}(\mathbf{u}, \mathbf{v}, p, \gamma) &= J(\mathbf{u}, \nabla \mathbf{u}; \gamma) \\ &+ \int_0^{t_f} \int_{0\Omega} (\mathbf{u}^a, \mathbf{v}^a, p^a, \phi^a) \mathbf{FS}(\mathbf{u}, \nabla \mathbf{u}, \mathbf{v}, \nabla \mathbf{v}, p, \nabla p, \phi, \nabla \phi, \gamma) d\Omega dt \end{aligned} \quad (19)$$

where the column set of monolithic equations for the fluid and solid is denoted by \mathbf{FS} . The objective function is denoted as $J(\mathbf{u}, \nabla \mathbf{u}; \gamma)$. For example, the domain integration of the time-varying compliance can be defined as follows:

$$J(\mathbf{u}, \nabla \mathbf{u}; \gamma) = \int_0^{t_f} \int_{0\Omega} \mathbf{S}^T \cdot \mathbf{T}_s d\Omega dt \quad (20)$$

The adjoint structural displacements and adjoint fluid velocities and pressures are denoted as \mathbf{u}^a , \mathbf{v}^a , and p^a , respectively. The adjoint phase-field variable is denoted by ϕ^a . The adjoint sensitivity analysis is performed using the calculus of variation.

$$\delta \mathcal{L} = 0 \quad (21)$$

The adjoint equations can be derived by setting the terms associated with the primal variables to zeros and with the proper boundary conditions (see [13] and references therein) as follows:

$$\frac{\partial \mathcal{L}}{\partial \mathbf{u}} \cdot \delta \mathbf{u} + \frac{\partial \mathcal{L}}{\partial \nabla \mathbf{u}} : \nabla \delta \mathbf{u} = 0 \quad (22)$$

$$\frac{\partial \mathcal{L}}{\partial \mathbf{v}} \cdot \delta \mathbf{v} + \frac{\partial \mathcal{L}}{\partial \nabla \mathbf{v}} : \nabla \delta \mathbf{v} = 0 \quad (23)$$

$$\frac{\partial \mathcal{L}}{\partial p} \cdot \delta p + \frac{\partial \mathcal{L}}{\partial \nabla p} : \nabla \delta p = 0 \quad (24)$$

$$\frac{\partial \mathcal{L}}{\partial \phi} \cdot \delta \phi + \frac{\partial \mathcal{L}}{\partial \nabla \phi} : \nabla \delta \phi = 0 \quad (25)$$

Note that the objective function is dependent only on the structural displacements, structural strains, and design variables, explicitly and implicitly. See [13] and references therein for the variational approach for sensitivity analysis of transient fluid problems. Indeed, the following sensitivity can be obtained by solving the above equations for the adjoint variables:

$$\frac{dJ}{d\gamma} = \frac{\partial J}{\partial \gamma} + \int_0^{t_f} \int_{0\Omega} (\mathbf{u}^a, \mathbf{v}^a, p^a, \phi^a) \frac{\partial \mathbf{FS}}{\partial \gamma} d\Omega dt \quad (26)$$

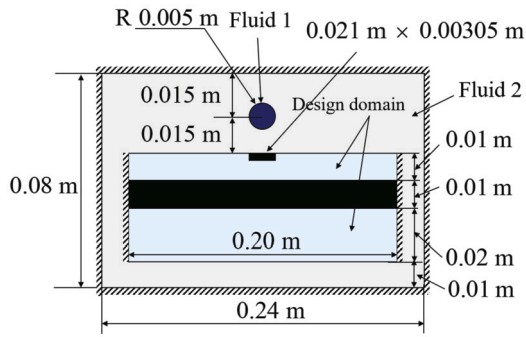


Fig. 2. Problem definition of Example 1 (Gravity: 9.81 m/s^2 in downward direction, Fluid: $\rho_1 = 1000 \text{ kg/m}^3$, $\mu_1 = 10 \text{ Pa s}$, $\rho_2 = 0.001 \text{ kg/m}^3$, $\mu_2 = 0.1 \text{ Pa s}$, Simulation time = 0:0.002:0.3, Structure: Plane strain assumption, Young's modulus = 10^6 N/m^2 , Poisson's ratio = 0.3, Density = 100 kg/m^3 , $\gamma_L = 0.1$, $\epsilon = 0.0005$, mesh in the design domain: 100 by (10+10+10), $\text{CFL} \leq 0.01$, $n = 3$, $n_s = 5$, $n_{filter} = 3$, $n_{pen} = 5$.)

3. Optimization examples

To show the validity of the present monolithic topology optimization for transient two-phase fluid-structure interaction, this section presents some examples with the dynamics of buoyant drop rising or falling through a fluid at low Reynolds numbers. The method of moving asymptotes (MMA) algorithm is employed as an optimization algorithm [35]. From an theoretical perspective, the aforementioned theory can be applied to a variety of flow problems. From an optimization perspective, several considerations arise, including the local optima issue, the convergence challenge, and the non-differentiability condition of the objective or the constraint functions due to the intricate interplay and behaviors of flow. Mitigating the non-differentiability and the convergence issues in the Navier-Stokes equation and the Phase-field equation requires the adoption of an appropriate combination of the analysis parameters and the simulation conditions, such as a stable time integration scheme, the stable wettability condition, the low CFL number condition, and mesh refinement. To tackle these challenges, the current study simplifies the simulation conditions. The analyses assume the simple falling or rising of drop with low Reynolds numbers. Structural displacements along the boundary increase the complexity and ambiguity in the finite element simulation as they should be interpreted as alterations of the analysis domain. Consequently, the external boundaries are assumed to be fixed to address these complexities. The Backward differentiation scheme is applied for the time integration.

3.1. Example 1: compliance minimization with dropping bubble

For the first example, the topology optimization problem considering the transient fluid-structure interaction effect is considered in Fig. 2. There is a droplet with $\rho_1 = 1000 \text{ kg/m}^3$ in the above rectangular slender solid non-design structural domain and whose density is larger than that of the ambient fluid, i.e., $\rho_2 = 0.001 \text{ kg/m}^3$. Due to the buoyancy and the gravity acting in this liquid, the droplet freely falls down and is deformed. It eventually contacts to the surface of the design domain and causes the time-varying structural compliance. For the sake of the simplification of the optimization problem, a flatten solid box is assumed at the vicinity of the contact domain, preventing the penetration of the droplet into the beneath design domain. We want to emphasize that the outside of the droplet is also another kind of fluid causing the movement of the design domain from a structural point of view and its movement contributes the objective function or the transient structural compliance but not as significantly as the heavier fluid. Due to the movements and influences of the two-phase flows and mainly due to the droplet, the structural domain transiently deforms down and then vibrates. Therefore, the objective of the optimization problem is set to distribute the

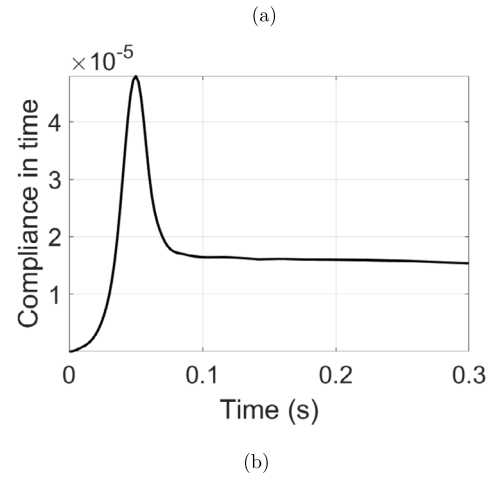
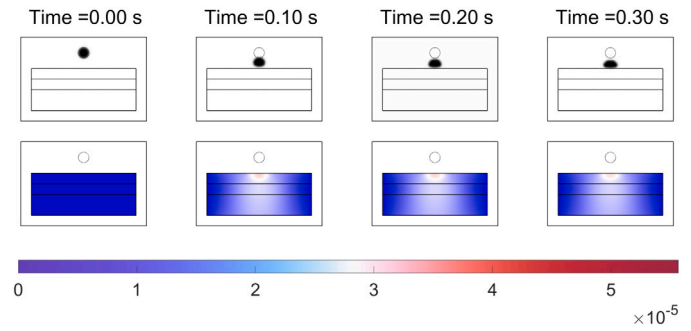


Fig. 3. Example 1. The initial response with an initial design $\gamma = 0.3$. (a) Top: the motions of the droplet and bottom: the norm of the structural displacements (maximum displacement: $5.57 \times 10^{-5} \text{ m}$) and (b) the time history of the compliance.

allowable mass inside the design domain to minimize the objective function which is set to the integration of the time varying compliance.

Before the optimization, the time varying compliance is measured for the simulation time and plotted in Fig. 3. Near 0.05 s (approximately $(2 \times \text{distance}/g)^{0.5}$), the droplet starts to contact the flat solid surface and naturally the structural compliance is increased and maximized. The design domain slightly vibrating after the contact, the oscillation of the time varying compliance is observed. The snap shots of the evolution of the droplets and the normalized structural vibrations at several times are shown in Fig. 3(a) and (b). With the present topology optimization scheme, it is possible to obtain the structure in Fig. 4. Upon first inspection, the overall layout is similar to an optimized layout of the compliance minimization for the structure with a force at the flat top of the solid box. Near at the upper part design domain of the horizontal bar, the supporting structure connecting the flatten solid box and the horizontal bar appears. At the bottom design domain and the sides of the horizontal bar, the topologically optimized supporting structures appear to effectively resist the fluid force due to the droplet. It is interesting to observe the comb-like structure at the bottom of the flatten solid box. To investigate this optimized structure further, the time-varying compliance values are computed in Fig. 4(b). As the time for the droplet contacting the surface is not changed, the peak is also observed near at 0.05 s. However, as a result of the optimized structure, the magnitude of the response is greatly diminished, decreasing by a factor of 10 as shown in Fig. 4. In addition, the oscillations of the values are also not observed that significantly minimizes the objective value which is the time integration of the time-varying compliance. This example shows that the present approach can be applied to find out an optimized layout considering the effect of the two-phase fluid-structure interaction phenomenon but the physical behavior of the flatten solid box should be investigated.

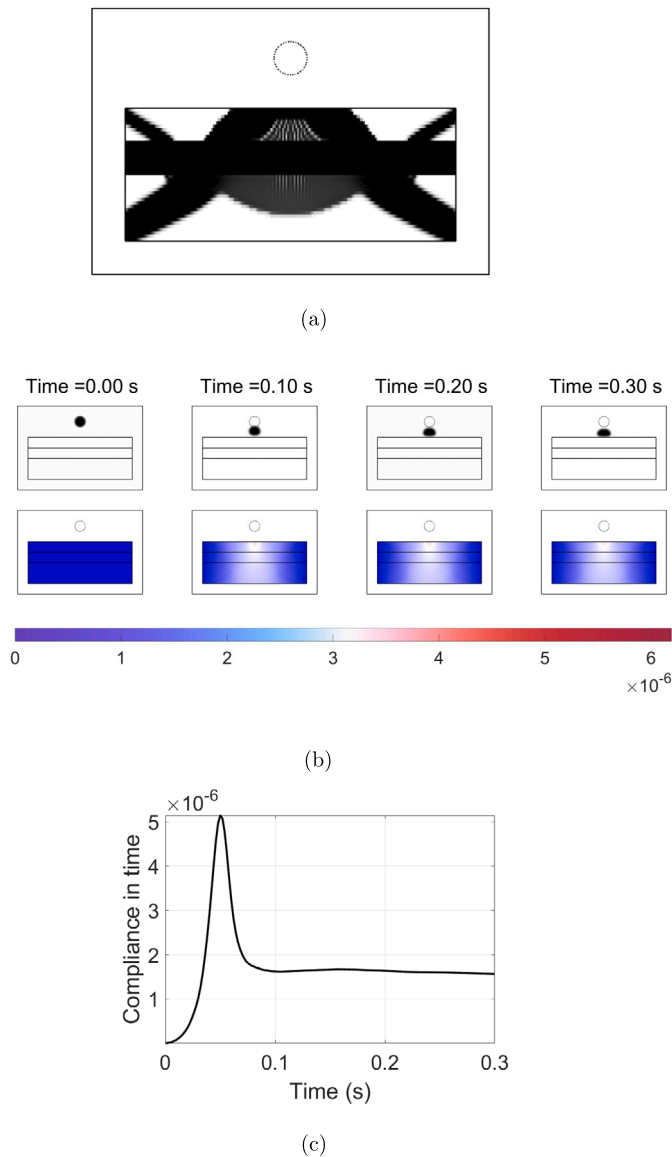


Fig. 4. Example 1. (a) Optimized design, (b) the responses, and (c) the time history of the compliance (maximum displacement: 6.1951×10^{-6} m).

To investigate the effect of the surface tension, the topology optimization problems with different surface tension values are solved in Fig. 5. The evolution of flow is dependent on the surface tension value and it is possible to obtain the different designs. Due to the local optima issue and the gray element issue, the objective values are almost same to each other.

For the next example, the flatten solid box fixing the time and the contact phenomenon between the droplet and the solid box is removed and not considered in the optimization formulation in Fig. 6. The challenge lies in the fact that the present optimization framework should determine not only the supporting structure but also the contact phenomenon, i.e., the contact time and the contact mechanism. Considering the balance between the kinetic energy and the potential energy, it is noticed that to minimize the objective function it is better to minimize the potential energy of the droplet that is the mass of the droplet time the gravity constant time the height. Therefore, a porous domain which partially minimizes the potential energy due to the gravity and partially minimizes the potential energy inside the design domain can be observed in Fig. 6(a). Interestingly, the fiber-like design can be obtained. Due to the intermediate variables and fiber-like designs, it is observed that the fluid can penetrate the porous domain but the fluid velocity is

slowly decreased that is crucial to minimize the reaction force. Fig. 6(b) and (c) show the fluid evolution and the structural motion. We tried to remove the intermediate design but it is our observation that the domain with the intermediate design variable works as a sponge to minimize the impact and the reaction force. However, in our present monolithic approach, we do not take into account the porous-like structure [36,37].

3.2. Example 2: compliance minimization with rising bubble

For the second example, the optimization problem in Fig. 7 is considered. By setting the similar domain of the first example but with the bottom droplet with a lighter density, the bubble is rising towards the design domain as shown in Fig. 8. As the bubble contacts at the bottom surface of the design domain, a slender box fixed as solid is moved and placed at the bottom of the design domain. With these conditions, the optimized layout in Fig. 9 can be obtained. Due to the gravity and the contact force, the structure whose stiffness is maximized can be obtained. The time varying compliance before and after the optimization are compared in Fig. 7 and Fig. 9. As observed in the first example, the responses are significantly minimized by the optimization. This example also shows that the present optimization algorithm can consider the effect of the two-phase flows. Then, the non-design solid box is removed and set as the design domain. To minimize the objective function, the porous design in Fig. 10 appears to minimize the total force exerting the design domain. The detailed responses are shown in Fig. 10. As observed, the porous domain appears in the contact region. This example also shows a typical situation of the two-phase flow coupled with the structure. One of the difficulties of this multiphysics system is to determine the optimized structure and the boundary between fluid and structure. The structural force is dependent on the design variable in addition to the fluid motion. Therefore, the penalization of the SIMP method may not be sufficient and some gray elements can exist.

3.3. Example 3: compliance minimization problem with two bubbles rising and sinking

For the last example, the influences of the density and size of bubbles are investigated by solving the four optimization problems. The first two problems are set with the two rising bubbles placed underneath the design domain and the fixed solid box located at the center of the design domain. Due to the buoyancy force, the two bubbles whose sizes are same at the first example and are heterogeneous at the second example rise toward the design domain. As the density of the rising bubble is set lighter than the density of the fluid embedding the two bubbles, the effect of the contacting of the two bubbles is not significant as shown in Fig. 11(b:right) and Fig. 12(b:right). Rather the initial movements of the two bubbles creating the motion of the containing fluid increase the structural compliance and determine the optimal designs. This aspect can be proven by the investigation of the symmetry of the designs in Fig. 11(a) and Fig. 12(a). Although the size of the right bubble in Fig. 12(a) is two time larger than that of the left bubble, the optimized design is almost symmetric that proves the effect of the bubbles is negligible compared with the effect of the heavier container fluid. On the other hand, the structural optimization problems considering the effect of the dropping fluid is considered in Fig. 13 and Fig. 14. As the bubbles whose diameters are same in Fig. 13 and are different in Fig. 14 and whose densities are set heavier than that of the containing fluid, the symmetric design is obtained in Fig. 13 where the antisymmetric design is obtained in Fig. 14. In Fig. 14, it can be observed that the force exerting on the surface of the right bubble is higher, some supporting structures stiffer than the supporting structures in the left design domain emerge in the right design domain. In addition, the porous structure observed in the previous example is not observed in this case. These designs show the importance of the consideration of the transient force due to the two-phase flow.

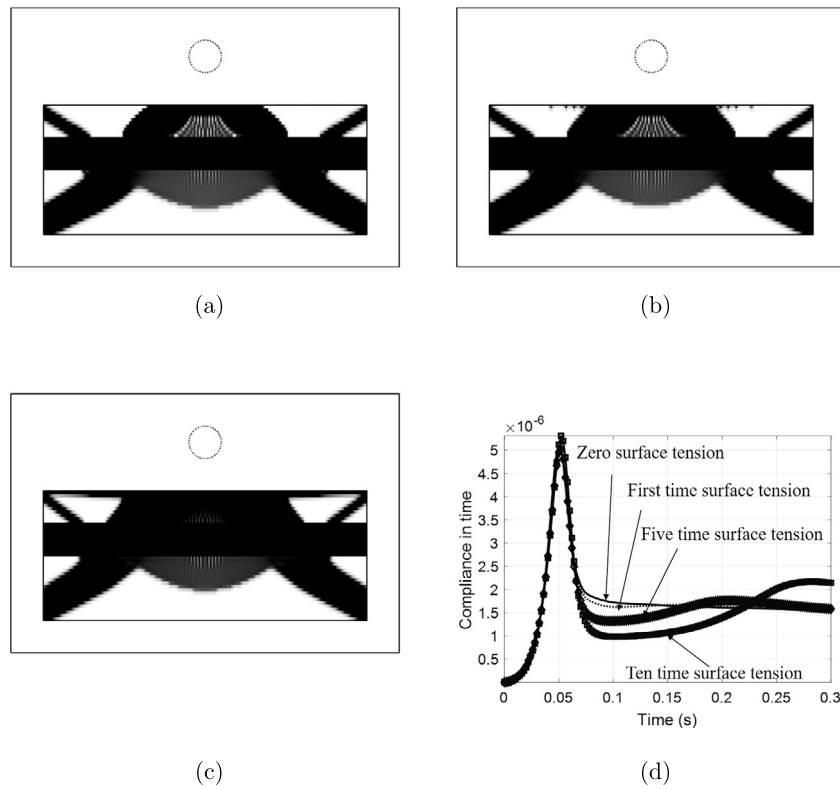


Fig. 5. Example 1. Optimized layouts with the different surface tension coefficient. (a) Zero surface tension, (b) five times surface tension, (c) ten times surface tension and (d) the compliance values.

4. Conclusions

This study has developed an analytical theory for a novel two-phase fluid-structure interaction system and a topology optimization scheme. Ascertaining and finding the optimized topologies for two-phase flow and structure interaction entails grappling with various interaction conditions including the surface tension effects in the fluid simulation, thus rendering the simultaneous optimization of fluid-structure domain and the coupling interaction condition a formidable challenge. Traditionally, there are two approaches to simulation or mathematical modeling of this interaction: the one-way coupling approach, which focuses on the influence of fluid on structure, and the two-way coupling approach, which additionally considers the influence of structural deformation on fluid. This multiphysics simulation presents considerable difficulties, especially when applying and implementing a topology optimization scheme without a predefined topology in prior. It is persistent to note that conventional simulation schemes typically require explicit boundary definitions between fluid (whether it's a single phase or two-phase flows) and structure, which can introduce theoretical and computational challenges when applying topology optimization to fluid-structure system. Moreover, as explicit boundaries are also necessary in two-phase flow simulation, the theoretical difficulty exists.

To address these difficulties, the present study introduces the following developments. Firstly, the monolithic design approach, which leverages the deformation tensor for fluid-structure interaction, is extended to accommodate one-way coupling. It is important to note that while the monolithic design approach can handle the two-way coupling, convergence issues may arise, particularly in two-phase flow simulation, even with the use of state-of-the-art simulation techniques. Thus, for the sake of simplifying the coupling simulation, one-way coupling is assumed that is one of the limitations of the present study. Due to several numerical difficulties such as the local optimum issue, the non-convergence and the dramatic change of flows the current study simplifies and limits the simulation conditions with the falling or rising of a drop with

low Reynolds numbers. To our best knowledge, this topic has not been considered in topology optimization. Secondly, two-phase flow simulation is conducted using the established phase-field method with the VOF method. In order to enhance numerical convergence in optimization and analysis, some adjustments and modifications are made to the phase-field equation that determines the type of fluid, taking into account the distribution of the design variables. The analysis of complex flow splitting and merging condition is possible. However, from an optimization point of view, these complex phenomena increase the computational time and the computation of the derivative considering complex flow behavior may not be possible. In addition, the present study only considers flow inside closed box as the structural displacement along the boundary means the alternation of the flow boundary condition.

With these advancements, it becomes possible to perform numerical simulations and topology optimization of two-phase flows. Based on the optimization results, several observations are made. When integrating structural compliance as the objective function with a mass constraint, the optimized layouts bear a resemblance to those obtained from compliance minimization problems. This is a logical outcome, as the motion of the two-phase flow exerts mechanical force on the structure, with the fluid stress serving as the origin. Consequently, the structural domain should possess greater stiffness to minimize structural compliance. Furthermore, it is observed that the motion of heavier fluid significantly influences the optimized layout. When lighter fluid moves upward due to buoyancy within heavier fluid, the predominant fluid-induced force stems from the heavier fluid. However, when the heavier fluid moves downward due to gravity, the fluid-induced force from the heavier fluid becomes a crucial factor in designing the optimized structure. Further scrutiny of the optimized layouts reveals the effectiveness of porous structures in minimizing the impact force at the interaction surface between the fluid and solid. One limitation of the present approach is its reliance on one-way coupling instead of two-way coupling. Therefore, in future research, it would be beneficial to develop a new numerical approach capable of incorporating the two-way coupling of two-phase

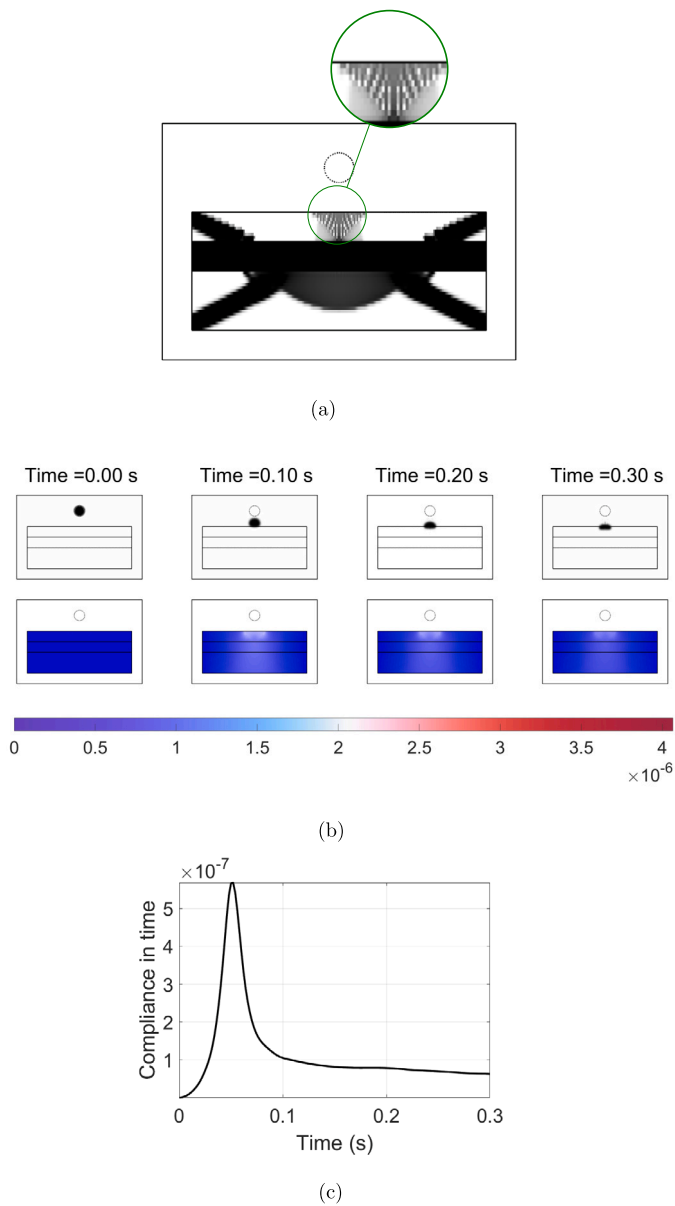


Fig. 6. Example 1. (a) Optimized design without the solid contact box, (b) the responses, and (c) the time history of the compliance (maximum displacement: 4.0659×10^{-6} m).

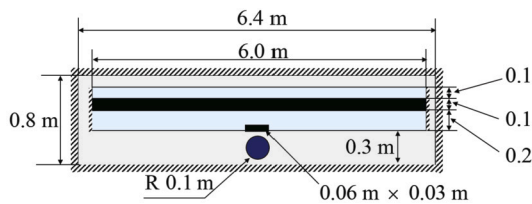


Fig. 7. Problem definition of Example 2 (Gravity: 9.81 m/s^2 in downward direction, Fluid: $\rho_1 = 1000 \text{ kg/m}^3$, $\mu_1 = 10 \text{ Pa s}$, $\rho_2 = 0.001 \text{ kg/m}^3$, $\mu_2 = 0.1 \text{ Pa s}$, $g = 9.81 \text{ m/s}^2$, Simulation time = 0:0.01:1, $\alpha_{\max} = 10^7$, Structure: Plane strain assumption, Young's modulus = 10^6 N/m^2 , Poisson's ratio = 0.3, Density = 100 kg/m^3 , $\gamma_L = 0.1$, $\epsilon = 0.0005$, mesh in the design domain 200 by (10+10+20), $\text{CFL} \leq 0.01$, $n = 3$, $n_s = 5$, $n_{\text{filter}} = 3$, $n_{\text{pen}} = 5$.)

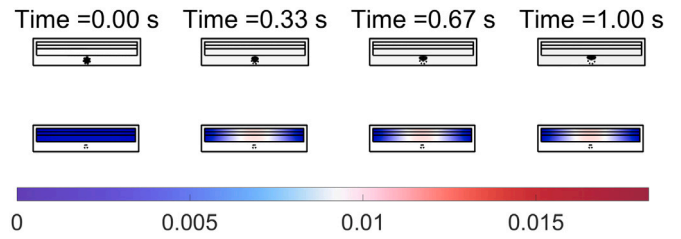


Fig. 8. The initial responses with an initial design $\gamma = 0.3$. (a) Top: the motions of the droplet and bottom: the norm of the structural displacements (maximum displacement: 0.0183 m) and (b) the time history of the compliance.

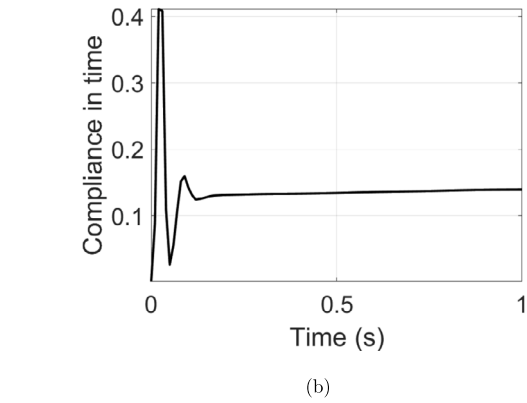


Fig. 9. Example 2. (a) Optimized design with solid box, (b) the responses, and (c) the time history of the compliance (maximum displacement: 0.0030 m).

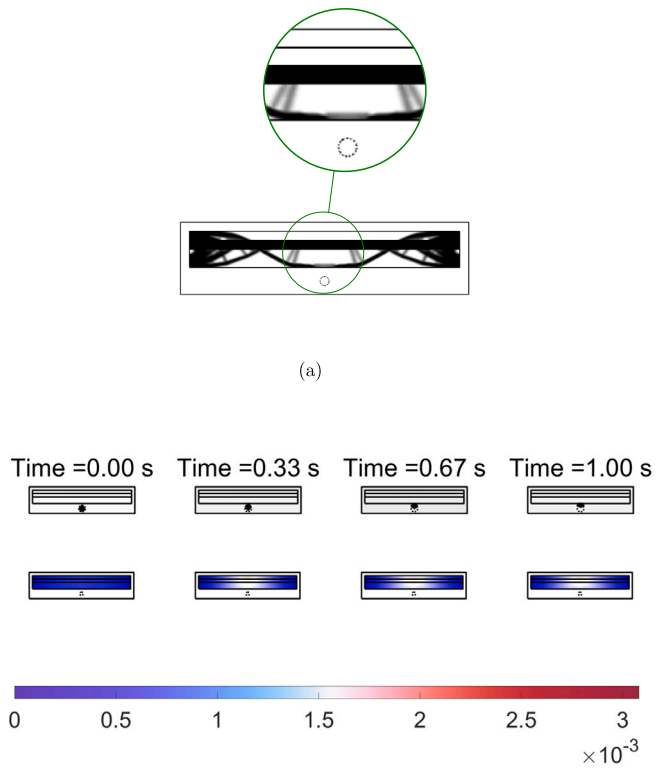


Fig. 10. Example 2. (a) Optimized design without solid box, (b) the responses, and (c) the time history of the compliance (maximum displacement: 0.0031 m).

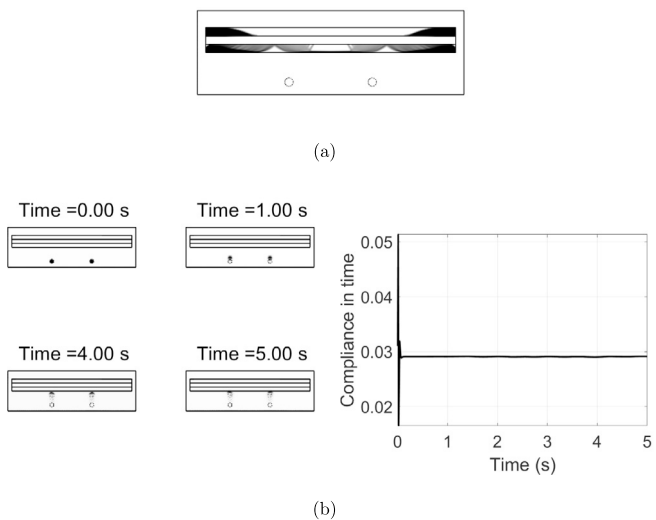


Fig. 11. Rising bubble example with the same radius ($\gamma_L = 0.02$, $\epsilon = 0.001$, time step: 0.01 s, CFL ≤ 0.01 s).

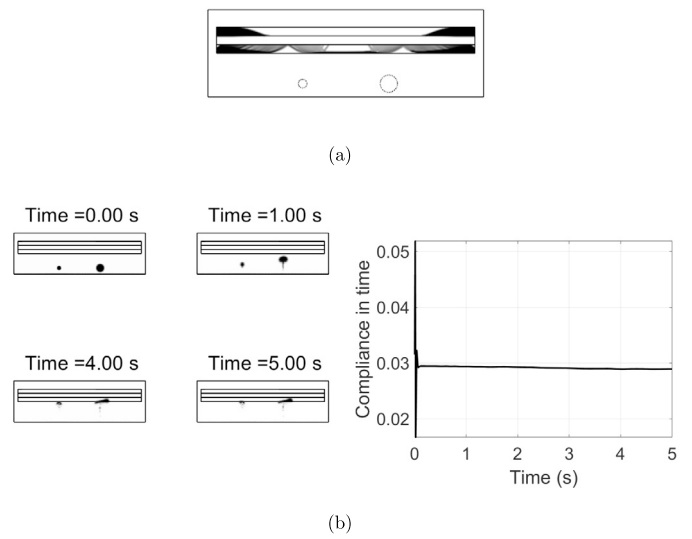


Fig. 12. Rising bubble example with the different radii.

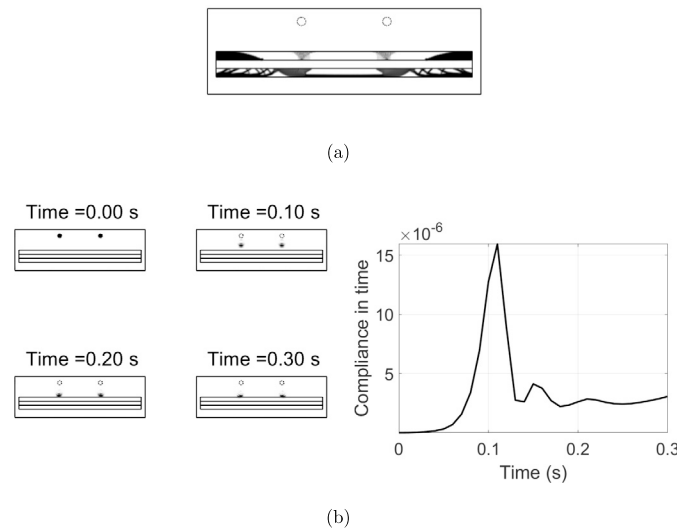


Fig. 13. Sinking bubble example with the same radius.

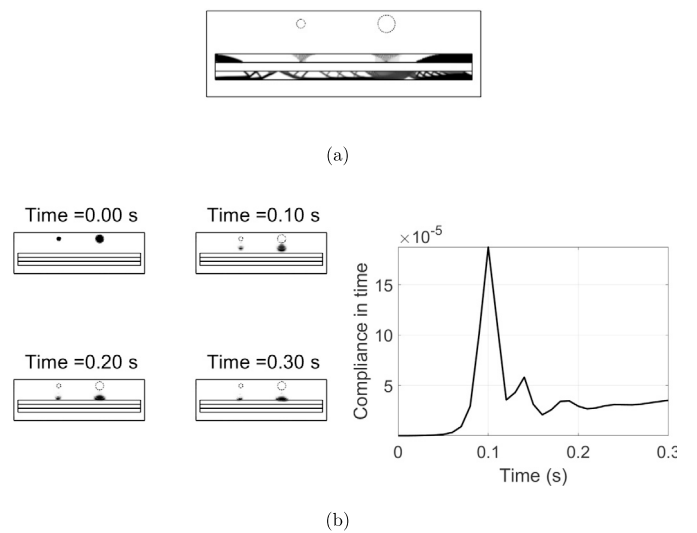


Fig. 14. Sinking bubble example with the different radii.

fluid-structure interaction systems. In addition, it is possible to include the mathematical formula to include the effect of the porous-like structure.

Funding information

This work was supported by a National Research Foundation of Korea (NRF) grant funded by the Korean government (MSIT) (RS-2024-00351611).

CRedit authorship contribution statement

Gil Ho Yoon: Writing – review & editing, Writing – original draft, Validation, Software, Methodology, Conceptualization.

Declaration of competing interest

The authors declare that they have no known competing financial interests or personal relationships that could have appeared to influence the work reported in this paper. Gil Ho Yoon

Data availability

Data will be made available on request.

References

- [1] Yoon GH. Topology optimization for stationary fluid-structure interaction problems using a new monolithic formulation. *Int J Numer Methods Eng* 2010;82(5):591–616.
- [2] Yin X, Zarikos I, Karadimitriou N, Raouf A, Hassanzadeh S. Direct simulations of two-phase flow experiments of different geometry complexities using volume-of-fluid (vof) method. *Chem Eng Sci* 2019;195:820–7.
- [3] Khan I, Wang M, Zhang Y, Tian W, Su G, Qiu S. Two-phase bubbly flow simulation using cfd method: a review of models for interfacial forces. *Prog Nucl Energy* 2020;125:103360. <https://doi.org/10.1016/j.pnucene.2020.103360>.
- [4] Tiwari S, Kuhnert J. Modeling of two-phase flows with surface tension by finite pointset method (fpm). Special Issue: *J Comput Appl Math* 2007;203(2):376–86. <https://doi.org/10.1016/j.cam.2006.04.048>.
- [5] Brackbill J, Kothe D, Zemach C. A continuum method for modeling surface tension. *J Comput Phys* 1992;100(2):335–54. [https://doi.org/10.1016/0021-9991\(92\)90240-Y](https://doi.org/10.1016/0021-9991(92)90240-Y).
- [6] Borrvall T, Petersson J. Topology optimization of fluids in Stokes flow. *Int J Numer Methods Fluids* 2003;77–107.
- [7] Dbouk T. A review about the engineering design of optimal heat transfer systems using topology optimization. *Appl Therm Eng* 2017;112:841–54.
- [8] Dede E. Multiphysics topology optimization of heat transfer and fluid flow systems. In: *Proceedings of the COMSOL conference*; 2009.
- [9] Joo Y, Lee I, Kim S. Efficient three-dimensional topology optimization of heat sinks in natural convection using the shape-dependent convection model. *Int J Heat Mass Transf* 2018;127:23–40.
- [10] Picelli R, Moscatelli E, Yamabe PVM, Alonso DH, Ranjbarzadeh S, dos Santos Gioria R, et al. Topology optimization of turbulent fluid flow via the tobs method and a geometry trimming procedure. *Struct Multidiscip Optim* 2022;65(34).
- [11] Okubo CM, Sá LF, Kiyono CY, Silva EC. A discrete adjoint approach based on finite differences applied to topology optimization of flow problems. *Comput Methods Appl Mech Eng* 2022;389:114406. <https://doi.org/10.1016/j.cma.2021.114406>.
- [12] Yan J, Xiang R, Kamensky D, Tolley MT, Hwang JT. Topology optimization with automated derivative computation for multidisciplinary design problems. *Struct Multidiscip Optim* 2022;65:114406.
- [13] Deng Y, Liu Z, Zhang P, Liu Y, Wu Y. Topology optimization of unsteady incompressible Navier–Stokes flows. *J Comput Phys* 2011;230(17):6688–708.
- [14] Chen XY. Topology optimization of microfluidics - a review. *Microchem J* 2016;127:52–61.
- [15] Alexandersen J, Aage N, Andreasen CS, Sigmund O. Topology optimisation for natural convection problems. *Int J Numer Methods Fluids* 2012;76(10):699–721.
- [16] Qian X, Dede EM. Topology optimization of a coupled thermal-fluid system under a tangential thermal gradient constraint. *Struct Multidiscip Optim* 2016;54(3):531–51.
- [17] Zhao X, Zhou M, Liu Y, Ding M, Hu P, Zhu P. Topology optimization of channel cooling structures considering thermomechanical behavior. *Struct Multidiscip Optim* 2019;59(2):613–32.
- [18] Yoon GH. Topological design of heat dissipating structure with forced convective heat transfer. *J Mech Sci Technol* 2010;24(6):1225–33.
- [19] Høghøj LC, Nørhave DR, Alexandersen J, Sigmund O, Andreasen CS. Topology optimization of two fluid heat exchangers. *Int J Heat Mass Transf* 2020;163:120543.
- [20] Duan X, Ma Y, Zhang R. Optimal shape control of fluid flow using variational level set method. *Phys Lett A* 2008;372(9):1374–9. <https://doi.org/10.1016/j.physleta.2007.09.070>. <https://www.sciencedirect.com/science/article/pii/S0375960107014223>.
- [21] Li H, Kondoh T, Jolivet P, Furuta K, Yamada T, Zhu B, et al. Three-dimensional topology optimization of a fluid–structure system using body-fitted mesh adaption based on the level-set method. *Appl Math Model* 2022;101:276–308.
- [22] Neofytou A, Yu F, Zhang L, Kim HA. Level set topology optimization for fluid-structure interactions. <https://arc.aiaa.org/doi/abs/10.2514/6.2022-2091>.
- [23] Li H, Kondoh T, Jolivet P, Nakayama N, Furuta K, Zhang H, et al. Topology optimization for lift–drag problems incorporated with distributed unstructured mesh adaptation. *Struct Multidiscip Optim* 2022;65.
- [24] Zhou S, Li Q. A variational level set method for the topology optimization of steady-state Navier–Stokes flow. *J Comput Phys* 2008;227(24):10178–95.
- [25] Jenkins N, Maute K. Level set topology optimization of stationary fluid-structure interaction problems. *Struct Multidiscip Optim* 2015;52(1):179–95.
- [26] Feppon F, Allaire G, Dapogny C, Jolivet P. Topology optimization of thermal fluid-structure systems using body-fitted meshes and parallel computing. *J Comput Phys* 2020;417:109574.
- [27] Yoon GH. Topological layout design of electro-fluid-thermal-compliant actuator. *Comput Methods Appl Mech Eng* 2012;209:28–44.
- [28] Yoon GH. Stress-based topology optimization method for steady-state fluid–structure interaction problems. *Comput Methods Appl Mech Eng* 2014;278:499–523.
- [29] Yoon GH, Kim MK. Topology optimization for transient two-phase fluid systems with continuous behavior. *Finite Elem Anal Des* 2023;225:104017. <https://doi.org/10.1016/j.finel.2023.104017>. Available from: <https://www.sciencedirect.com/science/article/pii/S016874X230001105>.
- [30] Picelli R, Ranjbarzadeh S, Sivapuram R, Gioria R, Silva E. Topology optimization of binary structures under design-dependent fluid-structure interaction loads. *Struct Multidiscip Optim* 2020;62:2101–16.
- [31] Picelli R, Vicente W, Pavanello R. Evolutionary topology optimization for structural compliance minimization considering design-dependent fsi loads. *Finite Elem Anal Des* 2017;135:44–55.
- [32] Siqueira LO, Cortez RL, Sivapuram R, Ranjbarzadeh S, dos R, Gioria S, et al. Topology optimization for stationary fluid–structure interaction problems with turbulent flow via sequential integer linear programming and smooth explicit boundaries. *Adv Eng Softw* 2024;190:103599. <https://doi.org/10.1016/j.advengsoft.2024.103599>. Available from: <https://www.sciencedirect.com/science/article/pii/S0965997824000061>.
- [33] Bernardi C, Maarouf S, Yakoubi D. Finite element discretization of two immiscible fluids with surface tension. hal-01128264. 2015.
- [34] Yoon GH. Topology optimization method with finite elements based on the $k-\epsilon$ turbulence model. *Comput Methods Appl Mech Eng* 2020;361:112784.
- [35] Svanberg K. The method of moving asymptotes – a new method for structural optimization. *Int J Numer Methods Eng* 1987;24(2):359–73.
- [36] Whitaker S. Flow in porous-media: 1. A theoretical derivation of Darcy’s-law. *Transp Porous Media* 1986;1:3–25.
- [37] Carrillo FJ, Bourg IC, Soulaire C. Multiphase flow modeling in multiscale porous media: an open-source micro-continuum approach. *J Comput Phys* 2020;X8:100073. <https://doi.org/10.1016/j.jcp.2020.100073>. Available from: <https://www.sciencedirect.com/science/article/pii/S2590055220300251>.